Published in final edited form as:

Mod Pathol. 2021 August ; 34(8): 1570–1587. doi:10.1038/s41379-021-00799-6.

Mesonephric and mesonephric-like carcinomas of the female genital tract: molecular characterization including cases with mixed histology and matched metastases

Edaise M. da Silva[#1], **Daniel J. Fix**[#1,2], **Ana Paula Martins Sebastiao**[1,3], **Pier Selenica**[1], **Lorenzo Ferrando**[1,4], **Sarah H. Kim**[5], **Anthe Stylianou**[5], **Arnaud Da Cruz Paula**[5], **Fresia Pareja**[1], **Evan S. Smith**[5], **Ahmet Zehir**[1], **Jason A. Konner**[6], **Karen Cadoo**[6], **Jorge S. Reis-Filho**[1], **Nadeem R. Abu-Rustum**[5], **Jennifer J. Mueller**[5], **Britta Weigelt**[1], **Kay J. Park**[1]

[1]Department of Pathology, Memorial Sloan Kettering Cancer Center, New York, NY, USA

[2]Department of Pathology, Hackensack University Medical Center, Hackensack, NJ, USA

[3]Department of Medical Pathology, Federal University of Parana, Curitiba, PR, Brazil

[4]Department of Internal Medicine, University of Genoa, Genoa, Italy

[5]Gynecology Service, Department of Surgery, Memorial Sloan Kettering Cancer Center, New York, NY, USA

[6]Department of Medicine, Memorial Sloan Kettering Cancer Center, New York, NY, USA

[#] These authors contributed equally to this work.

Abstract

Mesonephric carcinoma of the cervix is a rare tumor derived from Wolffian remnants. Mesonephric-like carcinomas of the ovary and endometrium, while morphologically similar, do not have obvious Wolffian derivation. Here, we sought to characterize the repertoire of genetic alterations in primary mesonephric and mesonephric-like carcinomas, in the distinct histologic components of mixed cases, as well as in matched primary tumors and metastases. DNA from microdissected tumor and normal tissue from mesonephric carcinomas (cervix, $n = 8$) and mesonephric-like carcinomas (ovarian $n = 15$, endometrial $n = 13$) were subjected to sequencing targeting 468 cancer-related genes. The histologically distinct components of four cases with

[✉]Britta Weigelt, weigeltb@mskcc.org; Kay J. Park, parkk@mskcc.org.

Author contributions KJP and JJM conceived the study, and KJP and BW supervised the study. KJP and DJF provided tissue samples and pathology data acquisition. KJP, DJF, and APMS conducted pathology review. EMdS, APMS, and AS performed sample processing. PS, LF, and AZ performed bioinformatics analyses. JAK, KC, and NRA-R provided patient information. Data acquisition, analysis, and interpretation was performed by EMdS, PS, LF, SHK, ADCP, FP, ESS, NRA-R, JSR-F, BW, and KJP. Manuscript drafting was performed by EMdS, BW, and KJP, and all authors edited and approved the final draft of the manuscript.
These authors jointly supervised this work: Britta Weigelt, Kay J. Park

Supplementary information The online version contains supplementary material available at https://doi.org/10.1038/s41379-021-00799-6.

Conflict of interest JSR-F reports receiving personal/consultancy fees from Goldman Sachs, REPARE Therapeutics and Paige.AI, membership of the scientific advisory boards of VolitionRx, REPARE Therapeutics and Paige.AI, membership of the Board of Directors of Grupo Oncoclinicas, and ad hoc membership of the scientific advisory boards of Roche Tissue Diagnostics, Ventana Medical Systems, Novartis, Genentech and InVicro, outside the scope of this study. NRA-R reports institutional grants from GRAIL and Stryker, outside the scope of this study. BW reports ad hoc membership of the scientific advisory board of REPARE Therapeutics, outside the scope of the submitted work. The remaining authors have no competing interests to declare.

mixed histology and four primary tumors and their matched metastases were microdissected and analyzed separately. Mesonephric-like carcinomas were underpinned by somatic *KRAS* mutations (25/28, 89%) akin to mesonephric carcinomas (8/8, 100%), but also harbored genetic alterations more frequently reported in Müllerian tumors. Mesonephric-like carcinomas that lacked *KRAS* mutations harbored *NRAS* (n = 2, ovary) or *BRAF* (n = 1, endometrium) hotspot mutations. *PIK3CA* mutations were identified in both mesonephric-like (8/28, 28%) and mesonephric carcinomas (2/8, 25%). Only mesonephric-like tumors harbored *CTNNB1* hotspot (4/28, 14%) and *PTEN* (3/13, 23%) mutations. Copy number analysis revealed frequent gains of chromosomes 1q and 10 in both mesonephric (87% 1q; 50% chromosome 10) and mesonephric-like tumors (89% 1q; 43% chromosome 10). Chromosome 12 gains were more frequent in ovarian mesonephric-like carcinomas, and losses of chromosome 9 were more frequent in mesonephric than in mesonephric-like carcinomas (both p = 0.01, Fisher's exact test). The histologically distinct components of four mixed cases were molecularly related and shared similar patterns of genetic alterations. The progression from primary to metastatic lesions involved the acquisition of additional mutations, and/or shifts from subclonal to clonal mutations. Our findings suggest that mesonephric-like carcinomas are derived from a Müllerian substrate with differentiation along Wolffian/mesonephric lines.

Introduction

Mesonephric carcinomas are rare malignant tumors of the uterine cervix, not related to human papillomavirus (HPV), that arise from mesonephric (Wolffian) duct remnants located deep in the cervical wall [1–7]. Mesonephric-like carcinomas arise in the uterine corpus, ovary, para-adnexal soft-tissue, or vagina [8–11] and display similarities to mesonephric carcinomas at the histomorphologic, immunophenotypic, and molecular levels, despite absence of obvious Wolffian origin [8, 12]. These tumors can present as pure adenocarcinomas or adenocarcinomas admixed with a sarcomatoid/spindle cell component [2, 6, 12–14], and have also been reported to occur in association with other histologic components such as ovarian low-grade serous carcinoma, serous borderline tumor, and endometrioid adenocarcinoma, suggesting transdifferentiation of Müllerian tumors into those with Wolffian/mesonephric lineage [15–18].

Histologically, mesonephric and mesonephric-like carcinomas are widely infiltrative and present a variety of architectural patterns, including tubular, solid, papillary, retiform and ductal, with cuboidal or columnar cells, increased mitotic activity and cytologic atypia [2]. The cytoplasm is usually minimal, while nuclei often have grooves and may show pseudoinclusions with nuclear overlap resembling features classically used to describe papillary thyroid carcinoma. Densely eosinophilic intraluminal secretions are frequently seen, most commonly with the tubular pattern, and solid areas may be spindled and frankly malignant (carcinosarcoma) which may be associated with heterologous elements, such as cartilage [10, 19]. A panel of immunohistochemical markers including expression of PAX8, GATA3, calretinin, CD10, TTF-1, and absence of estrogen and progesterone receptors (ER and PR), CEA, and p16 can be used to establish the diagnosis [6, 8, 20, 21].

Recent molecular studies have reported that both mesonephric and mesonephric-like carcinomas are underpinned by recurrent *KRAS* mutations and infrequent *PTEN* and *TP53* alterations, as well as microsatellite stability and frequent gains of chromosome 1q [3, 10, 11, 22, 23]. Alterations in chromatin remodeling genes such as *ARID1A, ARID1B*, and *SMARCA4*, not commonly mutated in other cervical cancers, have also been observed in mesonephric carcinomas [3], but not in mesonephric-like carcinomas. Conversely, *PIK3CA* mutations have been identified in mesonephric-like [11], but not in mesonephric carcinomas [3]. Given the high frequency of *PIK3CA* mutations in endometrioid endometrial carcinomas [24], a biological overlap of mesonephric-like carcinomas with carcinomas of both mesonephric and Müllerian (endometrioid) differentiation has been suggested. Whether mesonephric-like carcinomas represent mesonephric tumors that arise in the endometrium or ovary in the absence of mesonephric remnants, or whether they correspond to adenocarcinomas that derive from mesonephric-type differentiation of Müllerian lesions has yet to be elucidated [8]. In this study, we sought to define the repertoire of somatic genetic alterations in cancer-related genes in mesonephric and mesonephric-like carcinomas, and to determine the genetic profiles of histologically distinct components of mesonephric and mesonephric-like carcinomas with mixed histologic features, as well as of primary mesonephric/mesonephric-like carcinomas and their matched metastases.

Materials and methods

Case selection

Following Institutional Review Board approval, representative hematoxylin and eosin sections and formalin-fixed paraffin-embedded (FFPE) tissue blocks of a retrospective series of mesonephric ($n = 8$, cervical) and mesonephric-like carcinomas ($n = 28$; $n = 15$ ovarian and $n = 13$ endometrial) were retrieved from the pathology archives of Memorial Sloan Kettering Cancer Center. Cases were identified using the search term “mesonephric” in any part of the pathology report spanning the years 2008–2016. Cases were also identified prospectively during the course of this study which included metastases of primary tumors diagnosed prior to 2008. All cases were reviewed by three board-certified pathologists (KJP, DJF, and APMS) following the criteria put forward by the 2014 World Health Organization Classification of Tumors of Female Reproductive Organs [25] and as detailed above. Classic histology with supporting immunohistochemistry where required was utilized as the “gold standard” for patient inclusion in this study. For cases to be classified as mesonephric carcinosarcoma, the tumor had to be biphasic with a frankly malignant spindle cell component that was clearly separate and distinguishable from the carcinomatous component. After central pathology review and collection of clinicopathologic data, samples were anonymized.

For each patient, representative samples from the primary tumor or from the corresponding metastatic tumor, when primary tumor tissue was not available, were retrieved. Clinicopathologic characteristics, including age of the patient, tumor size, stage, and recurrence site(s) were retrieved from the patients’ medical records (Table 1). Tumor size was derived from the pathology report, either in the final diagnosis (if reported), or the gross

description. Tumors were staged according to the 2009 International Federation of Gynecology and Obstetrics criteria [26].

Whilst mesonephric and mesonephric-like carcinomas are histologically identical, criteria for inclusion in the study varied slightly depending on site of origin since the differential diagnoses are different at each anatomic site. Cervical mesonephric carcinomas were characterized by tumors based deep in the cervical stroma with varying degree of extension to the mucosal surface, consistent with origin in deeply placed mesonephric rests [25]. Immunohistochemistry for p16 was used to support the diagnosis when available. Mesonephric-like carcinomas were defined as tumors with classic histologic features of mesonephric carcinoma but occurring outside of the cervix [8]. In both the ovary and endometrium, immunohistochemical analyses were performed to confirm the diagnosis since the differential diagnosis includes endometrioid, clear cell, and serous neoplasms at both sites. From these anatomical sites, cases were only included if classic histology and appropriate immunohistochemical patterns were present (ER- and PR-negative, PAX8-positive, TTF-1/GATA3/CD10-positive to various degrees). The complete list of antibodies employed as well as the results are listed in Table 2.

Cases with mixed histology were also identified and confirmed with appropriate immunohistochemistry. Tumors of mixed histology were defined as those with a mesonephric component, as well as a distinct, separate histologically defined entity commonly seen in Müllerian tumors, such as mucinous, serous, and endometrioid types (Table 3). Mucinous tumors showed intracytoplasmic mucin globules with intestinal-type differentiation and concurrent immunohistochemical expression of at least one gastrointestinal-type marker (CK20, CDX2). Serous tumors showed cuboidal to columnar cells with round open chromatin, occasional cilia, hierarchical branching (in borderline tumors) and expression of WT1 and ER. Endometrioid histology was only accepted in the presence of confirmatory endometrioid features such as squamous differentiation.

In two ovarian mesonephric-like cases with mixed histology (OV21 and OV2), it was not possible to dissect the distinct components entirely due to the intimate association of the mesonephric-like and Müllerian components. In case OV21, the separately dissected components were pure mucinous vs mesonephric-like/mucinous together; and in case OV2, the mesonephric-like/serous borderline tumors were dissected together, given that pure mesonephric-like tumor areas could not be identified.

Immunohistochemistry

Immunohistochemical analysis was performed as part of the routine work-up of cases utilizing antibodies employed to establish the final diagnosis (Table 2). The scoring of the various markers was as follows: ER and PR: negative (0%), focal (≤5%), positive (>5%); PAX8, WT1, GATA3, TTF-1, HNF1beta, FOXL2: negative (0%), positive (any nuclear expression); CD10, CK7, CK20, CEA, vimentin, Napsin A: negative (0%), positive (any membranous or cytoplasmic expression); calretinin and inhibin: negative (0%), positive (any nuclear/cytoplasmic expression); p16: diffuse (strong positivity in >95% of cells), non-diffuse (<95% expression); p53: wild-type (heterogeneous nuclear expression), aberrant (strong nuclear expression in >90% of cells, complete absence of nuclear expression with

appropriate controls, cytoplasmic predominant expression). DNA mismatch repair proteins MLH1, PMS2, MSH2, and MSH6 were reported as retained (nuclear positivity for all four markers) or lost (specifying the specific proteins lost).

Microdissection and DNA extraction

Eight-μm-thick sections from representative FFPE tumor blocks from each case were stained with nuclear fast red and microdissected using a sterile needle under a stereomicroscope (Olympus SZ61) to ensure >80% tumor content, as previously described [27–29]. Histologically distinct tumor components were microdissected separately when possible. Genomic DNA of each tumor component and of matched normal tissue/blood was extracted using the DNeasy Blood and Tissue Kit (Qiagen) according to manufacturers' instructions.

Targeted massively parallel sequencing

Tumor and normal DNA samples from 8 mesonephric and 28 mesonephric-like carcinomas were subjected to targeted capture massively parallel sequencing using Memorial Sloan Kettering-Integrated Mutation Profiling of Actionable Cancer Targets (MSK-IMPACT) assay targeting 468 cancer-related genes [30], as previously described [27]. The median depth of coverage of tumor and normal samples was 649x (range 283×–1293×) and 450x (range 196×–834×), respectively. Sequencing data were processed as previously described [27, 28, 31]. In brief, somatic single nucleotide variants were detected by MuTect (v1.0) [32], and insertion and deletions (indels) by Strelka (v2.0.15) [33], VarScan2 (v2.3.7) [34], Lancet (v1.0.0) [35], and Scalpel (v0.5.3) [36]. Somatic mutations identified in the primary tumor or metastasis from a given patient or in one histologic component from a given tumor were subsequently interrogated in the matched respective primary/metastasis/other histologic component by manual inspection of BAM files using mpileup files (SAMtools mpileup; v1.2 htslib 1.2.1) [37]. FACETS [38] was employed to determine the copy number alterations (CNAs) and whether genes harboring a somatic mutation were targeted by loss of heterozygosity. The cancer cell fraction of each mutation was determined using ABSOLUTE (v1.0.6) [39], as previously described [28, 40]. Somatic mutations that were deleterious/loss-of-function affecting tumor suppressor genes or targeting a mutational hotspot in oncogenes were considered pathogenic. Mutational hotspots were assigned according to Chang et al. [41]. A maximum parsimony tree of the cervical mixed mesonephric and endometrioid carcinoma CX26 was built based on the non-synonymous somatic mutations and gene CNAs, as described [42].

Statistical analysis

The frequencies of somatic mutations affecting cancer genes in mesonephric and mesonephric-like carcinomas were compared using Fisher's exact test. Fisher's exact test and Chi-Square test were used for comparison of categorical variables, and Mann–Whitney U test for continuous variables. Two-tailed p values <0.05 were considered significant.

Results

Clinicopathologic features of mesonephric and mesonephric-like carcinomas

In this study a total of 36 cases were included: 8 cervical, 15 ovarian, and 13 endometrial. Cervical tumors comprised mesonephric carcinomas ($n = 6$), a mesonephric carcinosarcoma ($n = 1$), and a mixed mesonephric and endometrioid carcinoma ($n = 1$). Tumors in the ovary and endometrium comprised mesonephric-like carcinomas ($n = 9$ and $n = 11$, respectively), mesonephric-like carcinosarcomas ($n = 1$ and $n = 2$, respectively) and mesonephric-like carcinomas with mixed histological components ($n = 5$ in ovary; Tables 1 and 3). Two of the ovarian mixed tumors had a mucinous borderline component, and three a low-grade serous neoplasm (carcinoma and/or borderline tumor).

The median age at diagnosis was not significantly different between patients with mesonephric carcinomas (60.5 years, range 30–75) and mesonephric-like carcinomas (61 years, range 36–76; ($p = 0.88$, Mann–Whitney *U* test, Table 1). Also, no significant differences in stage at diagnosis ($p = 0.12$, Chi-Square test) or tumor size ($p = 0.43$, Mann–Whitney *U* test) were observed between mesonephric and mesonephric-like tumors. Seventy-five percent (6/8) of the mesonephric and 78% (22/28) of the mesonephric-like tumors developed metastatic disease ($p > 0.05$, Fisher's exact test), with the most frequent sites of metastases including the abdomen/pelvis (36%), lung (36%), liver (14%), and vagina (11%; Table 1).

Somatic genetic alterations in mesonephric and mesonephric-like carcinomas

Targeted sequencing revealed that mesonephric carcinomas harbored a median of 5.5 (range 3–9) non-synonymous somatic mutations in the 468 genes analyzed, and mesonephric-like carcinomas in the ovary and endometrium displayed a median of 4 (range 1–9) non-synonymous mutations ($p = 0.17$, Fisher's exact test, Supplementary Table S1). *KRAS* was the most recurrently mutated gene, with 100% (8/8) of mesonephric carcinomas, 87% (13/15) of ovarian and 92% (12/13) of endometrial mesonephric-like carcinomas harboring *KRAS* somatic mutations (Fig. 1A and Supplementary Table S1). The majority of these mutations affected the hotspot codons 12 and 13 of *KRAS* (G12D, G12V, G12C, G12A, and G13D), except for cervical case CX67, which harbored an in-frame insertion (p.G13dup). Of note, the two ovarian (OV74 and OV2) and one endometrial (EM76) cases that lacked *KRAS* mutations harbored other mutations in the MAPK pathway, namely *NRAS* p.Q61R hotspot mutations (both ovarian cases) or *BRAF* p.N581S and *RRAS2* p.Q72L hotspot mutations (endometrial EM76; Fig. 1A). One metastatic endometrial mesonephric-like case (EM72) harbored *KRAS* G13D mutation co-occurring with hotspot mutations affecting *RRAS2* (Q72L) and *TP53* (I254N). *PIK3CA* hotspot mutations were identified in two mesonephric carcinomas (2/8, 25%; p.R88Q hotspot; pathogenic p.I1058F), five ovarian mesonephric-like tumors (5/15, 33%), and three endometrial mesonephric-like carcinomas (3/13; 23%; 2/3 hotspot mutations; Fig. 1A and Supplementary Table S1). In contrast, *CTNNB1* hotspot mutations were restricted to mesonephric-like tumors, present in 7% (1/15) and 23% (3/13) of the ovarian and endometrial tumors, respectively, as well as the endometrioid component of the mixed mesonephric-endometrioid cervical carcinoma CX26. Similarly, somatic mutations affecting genes involved in the ubiquitin-proteasome system

such as *SPOP* (4/15, 27%; 1/13, 8%), *FBXW7* (1/15, 7%; 1/13, 8%) and *FANCA* (1/15, 7%; 1/13, 8%), commonly altered in endometrial cancers [24], were identified exclusively in ovarian and endometrial mesonephric-like tumors, respectively. Finally, we found mutations in other cancer-related genes to be restricted to endometrial mesonephric-like carcinomas, including *AMER1* (2/13), *EPHA3* (2/13), *RRAS2* (2/13), *TP53* (1/13), and *PTEN* (3/13), the latter being present in a mesonephric-like carcinosarcoma (EM63) and two mesonephric-like carcinomas (EM1 and EM64).

Copy number analysis revealed that mesonephric and mesonephric-like carcinomas displayed moderate levels of genomic instability with no recurrent amplifications or homozygous deletions (Fig. 1B). Irrespective of site, recurrent gains of 1q (32/36, 89%), chromosome 10 (16/36, 45%), and chromosome 2 (13/36, 36%; all $p > 0.05$, Fisher's exact test) were found. Gains of chromosome 12 were significantly more frequent in ovarian mesonephric-like carcinomas (10/15, 67%) than in mesonephric (2/8, 25%) or endometrial mesonephric-like tumors (2/13, 15%; $p = 0.013$, Fisher's exact test). Loss of chromosome 9 was significantly more frequent in mesonephric (4/8, 50%) than in mesonephric-like carcinomas (ovary 1/15, 7%; endometrium 1/13, 8%; $p = 0.016$, Fisher's exact test).

Molecular characterization of mesonephric and mesonephric-like carcinomas with mixed histology

Six of the 36 mesonephric and mesonephric-like carcinomas included in this study displayed mixed histology (Table 1). To characterize the molecular alterations in four of these mixed cases, histologically distinct tumor components from one cervical (CX26) and three ovarian cancers (OV21, OV74, and OV75) were separately microdissected and subjected to MSK-IMPACT sequencing (Figs. 2 and 3 and Table 3).

Cervical mixed carcinoma—CX26 was a cervical mesonephric carcinoma mixed with an endometrioid carcinoma, negative for high-risk HPV, whereby the mesonephric component was composed of two morphologically distinct areas—an intramural component showing classic tubular growth pattern with dense eosinophilic intraluminal secretions located deep in the cervical wall, and an exophytic component comprised of long slender branching papillae with anastomosing "villoglandular" pattern. The endometrioid carcinoma was composed of confluent cribriform glands lined by columnar cells with round, vesicular nuclei with prominent nucleoli and associated squamous differentiation with keratinization (confirmatory endometrioid feature). The endometrioid component was located in the cervical stroma at the center of the tumor between the two mesonephric components, separated by a discrete border. Immunohistochemical analysis of the different components revealed that the mesonephric carcinoma was completely negative for ER and PR, whereas the endometrioid carcinoma showed patchy strong positivity for these markers, supporting the different histologies of the two components. TTF-1 and GATA3 were negative in both components (Table 2 and Supplementary Fig. S1A–F). These three histologically distinct areas were separately analyzed (Fig. 2 and Table 3). We observed that the three components harbored a clonal truncating mutation in the chromatin remodeling gene *ARID1A* p.S664∗, a subclonal *ASXL1* p.E558Tfs∗4 mutation, gain of chromosome 17q, and loss of chromosome 17p. A subclonal *PALB2* (p.S326L) mutation in the intramural mesonephric

component was found to become clonal in the exophytic mesonephric and endometrioid components. A clonal *KRAS* p.G12D hotspot mutation was found to be restricted to the intramural and exophytic mesonephric components, whereas only the endometrioid component harbored a clonal *CTNNB1* p.G34R hotspot mutation (Fig. 2). Consistent with this, we observed that only the intramural and exophytic mesonephric components had gain of chromosome 16, whereas the endometrioid component harbored a chromosome 12 gain, which was not present in the other two mesonephric components (Fig. 2). These findings suggest that the different lesions shared a common ancestor, with independent evolution in the mesonephric and endometrioid components (Fig. 2B).

Ovarian mixed tumors—Genomic analysis of the different components was also performed in two mesonephric-like with mucinous borderline tumors (OV75 and OV21) and one mesonephric-like with serous borderline tumor/low-grade serous carcinoma (OV74).

OV75 was a 10.3 cm unilateral mixed mesonephric-like carcinoma and mucinous borderline tumor affecting the right ovary. Gross sections showed a multilocular cystic mass that was 30% solid and 70% cystic. Histologically, the cystic portion of the mass was lined by gastrointestinal-type mucinous epithelium that ranged from a single layer of cells containing abundant gastrointestinal-type mucin, including goblet cells, and round to ovoid basally located nuclei (consistent with mucinous cystadenoma) to finger-like projections lined by similar cells (borderline tumor; Fig. 3A). The solid areas were a mixture of mucinous cystadenofibroma intimately admixed with scattered foci of mesonephric-like carcinoma with variable architecture, including tubular with eosinophilic intraluminal secretions, glandular and glomeruloid (Fig. 3A). Immunohistochemical analysis demonstrated that the mesonephric-like carcinoma and the mucinous tumor had distinct expression patterns, while showing some unexpected overlap. The mesonephric-like component was positive for CK7, PAX8 (strong intensity), GATA3 and TTF-1, while negative for CK20, WT1, and PR; ER was focally weakly positive. As expected, the mucinous tumor was positive for CK7, CK20, PAX8 (weak intensity), and lacked ER, PR, and WT1 expression. Unexpectedly, however, the mucinous component was also positive for GATA3 and TTF-1, though with an intensity weaker than that found in the mesonephric-like component (Supplementary Fig. S1G–K). DNA mismatch repair proteins (MLH1/PMS2, MSH2/MSH6) were retained and p53 showed heterogeneous wild-type expression in both components. There were a few foci of nodular expansion of pure mesonephric-like carcinoma amenable to microdissection for sequencing. The mucinous borderline tumor was also microdissected for genomic analysis and the results were compared. Both components shared similar copy number alterations (CNAs), as well as clonal *CD79A* p.T140N, *NOTCH2* p.V1633I and *POLD1* p.I927L missense mutations (Fig. 3A). Both components harbored a subclonal *PIK3CA* p.P539R hotspot mutation, as well as a *KRAS* p.G12V hotspot mutation. Private mutations were detected in each component separately, *SETD8* p.A21V mutation in the mesonephric-like and *PIK3R1* p.R386G mutation in the mucinous borderline component.

Case OV21 was also unilateral limited to the right ovary and consisted of a mesonephric-like carcinoma intimately admixed with a mucinous borderline tumor/cystadenofibroma (Fig. 3B). Unlike OV75, the immunohistochemical profiles of the two components were distinct: the mesonephric-like carcinoma was positive for PAX8, GATA3, TTF-1 with rare PR

expression, negative for ER, CK20, and WT1; the mucinous tumor was positive for PAX8 and CK20, negative for GATA3 and TTF-1 (Supplementary Fig. S1L–P). Whilst the pure mucinous borderline tumor was microdissected and separately analyzed, the mesonephric component was too intimately admixed with the mucinous tumor for microdissection and, therefore, the mesonephric-like carcinoma and mucinous tumor (cystadenofibroma) were analyzed together in the second sample of this case, with greater cellular contribution from the mesonephric-like component (Fig. 3B). Both samples shared clonal *KRAS* p.G12D hotspot and *SPOP* p.M117T missense mutations, and gains of chromosomes 10 and 12 and 1q. Subclonal *CTNNB1* p.D32V/p.T41A and *AKT1* p.E17K hotspot mutations were found only in the mixed mesonephric/mucinous component, whereas the mucinous borderline tumor had a private subclonal *NOTCH3* p.F1327S missense mutation.

OV74 was composed of mesonephric-like and low-grade serous carcinoma arising in a background of serous borderline tumor. Surface involvement was detected in both ovaries and was present in the form of a serous borderline tumor composed of long slender papillae with hierarchical branching lined by cuboidal to columnar cells, some with cilia along the luminal edge. The borderline tumor in the right ovary showed focal micropapillary features with epithelial proliferation not supported by underlying fibrovascular stroma, some of which merged to form a microcystic configuration. The low-grade serous carcinoma component was focal in both ovaries, mostly along the periphery and in the hilum. The mesonephric-like component was predominant in the left ovary, present as a solid nodular expansion in the ovarian cortex, separate from the serous elements (Supplementary Fig. S1Q–U). Widespread metastases by both the mesonephric-like and low-grade serous carcinomas were found (Table 1), with the majority of sites (including falciform ligament, peritoneum, and colon) containing only mesonephric-like carcinoma, whereas the lesions affecting the omentum, Gerota's fascia, and diaphragm contained both. The pleura was the sole site containing only low-grade serous carcinoma. The focus of serous borderline tumor on the right ovarian surface and the deposit of mesonephric-like carcinoma in the right fallopian tube were microdissected and sequenced separately (Fig. 3C). Both components harbored few somatic mutations and shared a clonal *NRAS* p.Q61R hotspot mutation and several copy CNAs including a 1q gain, losses of chromosomes 4 and 18 (Fig. 3C). The acquisition of a subclonal *HIST1H3I* p.G103R mutation and several CNAs (including gains of chromosomes 6p and 17) in the mesonephric-like component, suggests that the mesonephric-like carcinoma arose from the low-grade serous neoplasm, consistent with a tumor of Müllerian origin that evolved along a mesonephric lineage.

Molecular characterization of primary mesonephric and mesonephric-like carcinomas and their matched metastases

Representative samples from four primary tumors and their respective distant metastases (CX8, OV2, EM61, and EM52) were independently subjected to MSK-IMPACT sequencing (Table 3). Chromosome 1q gains were present in the primary tumor and the respective metastasis in the four cases analyzed (Fig. 4).

The primary mesonephric carcinoma of the cervix (CX8) and the matched brain metastasis were genomically unstable and had a relatively high number of mutations as compared to the

other cases in this study (Fig. 4A). The primary cervical lesion and brain metastasis shared a clonal *KRAS* p.G12D hotspot mutation and subclonal *ARID1A* (p.X1368_splice and p.P1423Rfs∗18) mutations. A shift in the clonality of mutations was observed in the progression: *BLM* p.V958M, *MTOR* p.T1149A, and *PIK3CA* p.R88Q hotspot mutations were found to be subclonal in the primary tumor and came to become clonal in the brain metastasis (Fig. 4A). Both, the primary tumor and brain metastasis underwent parallel evolution and acquired somatic mutations restricted to the primary mesonephric carcinoma, including an *NTRK3* p.A830G missense mutation, or to the brain metastasis, including a clonal *SF3B1* p.R625C hotspot mutation.

Case OV2 was an ovarian mesonephric-like carcinoma admixed with serous borderline tumor, which recurred in the pelvis (Supplementary Fig. S1V–Z). Both primary mesonephric-like carcinoma/serous borderline tumor and the matched pelvic metastasis harbored clonal *NRAS* Q61R hotspot mutation (Fig. 4B). Clonal *ATR* p.A2014V and subclonal *TNFAIP3* p.F7831 missense mutations were acquired in the progression of the disease from primary tumor to metastasis.

Both the primary mesonephric-like carcinoma in the endometrium and its corresponding abdominal wall metastasis of EM61 harbored clonal *KRAS* p.G12V hotspot mutations and similar patterns of CNAs. Also in this case, in the progression from primary to metastasis, additional mutations were acquired, including *MAP3K13* (p.G100R), *MET* (p.L1212R), and *MAPK3* (p.E358V) missense mutations, not present in the primary tumor (Fig. 4C).

Finally, we analyzed the primary endometrial mesonephric-like carcinoma EM52 and its matched lung metastasis; both harbored a clonal *KRAS* p.G12D hotspot mutation and gain of 1q. No additional somatic mutations were found in the 468 key cancer genes analyzed (Fig. 4D).

Discussion

Here we report on the repertoire of genetic alterations of cancer-related genes in a series of mesonephric carcinomas of the cervix, and mesonephric-like carcinomas of the ovary and endometrium, as well as histologically distinct components of mesonephric and mesonephric-like carcinomas with mixed histology, and primary mesonephric/mesonephric-like carcinomas and their matched metastases. We demonstrate that mesonephric-like carcinomas are underpinned by activating *KRAS* mutations akin to mesonephric carcinomas, but also harbor genetic alterations that are frequently reported in Müllerian tumors, such as *PIK3CA, PTEN*, and *CTNNB1* mutations.

Consistent with previous studies, *KRAS* activating mutations, mostly affecting the hotspot codons 12 and 13, were found in the vast majority of mesonephric (100%) and mesonephric-like carcinomas (87% ovarian and 92% endometrial) [3, 10, 11, 23, 43]. In the absence of *KRAS* hotspot mutations, mesonephric-like carcinomas were found to harbor hotspot mutations in other RAS/RAF family genes such as *NRAS, BRAF*, and/or *RRAS2*. As expected, *KRAS* and *NRAS/BRAF* mutations were mutually exclusive in both mesonephric and mesonephric-like carcinomas. These data provide evidence to suggest that RAS/MAPK

pathway alterations may be drivers of both mesonephric and mesonephric-like carcinomas. Recent studies have reported promising results with therapies targeting RAS [44–46] and PI3K/AKT/mTOR pathway [47] in other malignances. Further studies to investigate the therapeutic effect of targeting the RAS/MAPK signaling pathway in the absence and presence of PI3K pathway alterations in mesonephric and mesonephric-like carcinomas are warranted.

A subset of mesonephric-like carcinomas with RAS pathway alterations were found to harbor concurrent *PIK3CA* (5/15, 33% ovarian and 3/13, 23% endometrial) and/or *PTEN* hotspot mutations (3/13, 23% endometrial). Notably, two cervical mesonephric carcinomas harboring *KRAS* hotspot mutations also harbored a concurrent *PIK3CA* mutation. These findings differ from those of Mirkovic et al. [3], who reported no *PIK3CA* hotspot mutations in 13 cervical mesonephric carcinomas. Genetic alterations affecting *PTEN* and *PIK3CA* are commonly found in endometrial and other types of cervical adenocarcinomas, while *TP53* mutations are found in the vast majority of endometrial serous carcinomas, but not in mesonephric and other cervical adenocarcinomas. Based on these observations, it has been suggested that the lack of *PIK3CA, PTEN*, and *TP53* mutations, in combination with the presence of *KRAS* or *NRAS* mutations, could be employed to favor a mesonephric carcinoma over another histologic type of endometrial or endocervical adenocarcinoma [3, 48–50]. However, it is now clear from this as well as other studies [10, 11, 22] that a subset of mesonephric-like carcinomas harbor mutations commonly found in Müllerian tumors, such as *PTEN, PIK3CA*, and *CTNNB1*, suggesting that these mesonephric-like carcinomas are Müllerian derived and therefore, the presence of mutations more typically seen in Müllerian carcinomas does not exclude the diagnosis of mesonephric-like carcinoma.

All of these findings provide additional support to the recently proposed concept that mesonephric-like carcinomas are derived from Müllerian origins through a process of transdifferentiation. Whilst in the cervix, it is well established that mesonephric remnants deep in the cervical wall serve as the nidus from which tumors arise, the origin of mesonephric-like carcinomas is less clear since the existence of mesonephric remnants in the corpus and ovary is questionable. There have been a few case reports of mesonephric-like carcinomas of the endometrium and ovary arising in association with other more conventional Müllerian tumors: a mixed endometrioid and mesonephric-like carcinoma in the endometrium and three cases of mesonephric-like carcinoma mixed with low-grade serous neoplasms [15–18]. These reports showed identical *KRAS* or *NRAS* mutations in both components and postulated that rather than arising from mesonephric remnants, these tumors have Müllerian origins with differentiation along mesonephric lines. Here we report six additional mixed cases in the cervix and ovary, and microdissection of the different components was performed in four of these cases, including a rare cervical mesonephric mixed with endometrioid carcinoma and two ovarian mucinous borderline tumors mixed with mesonephric-like carcinoma. Analyses of these four cases demonstrated that the histologically distinct components of mixed mesonephric (cervical, $n = 1$) and mesonephric-like (ovarian, $n = 3$) carcinomas generally harbored similar patterns of genetic alterations, providing evidence to support their clonal relatedness, but in addition demonstrating that each component harbored private mutations.

Based on the presence of somatic genetic alterations in common between the histologically distinct components of the two mixed mesonephric and mucinous borderline tumors, the most parsimonious explanation for our findings is that these do not constitute collision tumors. Instead, our findings demonstrate that the two histologically distinct components are clonally related. Based on the clonal deconvolution analyses performed, in OV75, the mesonephric-like component may have constituted the substrate from which the mucinous component developed, given that the subclonal *KRAS* and *PIK3CA* mutations present in the mesonephric-like component came to become clonal in the mucinous component. We cannot rule out, however, that there was mucinous tumor intermixed with the mesonephric-like component subjected to sequencing, leading to the detection of "subclonal" mucinous tumor-derived mutations in the mesonephric-like component. In case OV21, the directionality of progression could not be inferred based on the repertoire of genetic alterations present, given that the mutations shared between the mixed mesonephric-like/mucinous and mucinous components were clonal in both and that the copy number profiles were strikingly similar. Consistent with the notion of the clonal relatedness of both components in the two tumors analyzed, areas where the two components merged and shared overlapping immunohistochemical expression patterns were detected.

The one cervical mixed case in our series (CX26) is the second case of mesonephric carcinoma mixed with another component reported in the literature to date. While the case in our current series featured mesonephric combined with endometrioid carcinoma, the case previously reported by our group was a mesonephric carcinoma combined with a high-grade neuroendocrine carcinoma where the two components were also clonally related and negative for high-risk HPV [51]. In the current case, the mesonephric portion was comprised of two histologically and geographically distinct areas, a tubular intramural component and a "villoglandular" exophytic component; in between these two areas was an endometrioid carcinoma with squamous differentiation that abutted both the intramural and exophytic mesonephric tumors. All three areas showed the same *ARID1A* mutation, demonstrating their clonal relatedness. The *KRAS* hotspot mutation was present only in the mesonephric tumor (both components), whereas only the endometrioid carcinoma harbored a *CTNNB1* mutation. This case is interesting for several reasons: (1) cervical mesonephric carcinoma mixed with another histologic type is extremely rare, with only one prior publication describing this phenomenon [51]; (2) mesonephric and endometrioid carcinomas of the cervix are both rare tumors, endometrioid carcinomas comprising <1% of all cervical carcinomas [52], such that the occurrence of both tumors in a single case is quite extraordinary; (3) The mesonephric and endometrioid components shared the same *ARID1A* mutation confirming clonality, while acquisition of independent mutations, *KRAS*, and *CTNNB1*, defined their divergent differentiation.

The analyses of primary and paired metastatic tumors demonstrated that mutations affecting RAS family genes were clonal throughout the metastatic process, and identified alterations restricted either to the primary or metastatic tumor in a given case. Furthermore, we found that the progression from primary to metastatic lesions involved the acquisition of additional somatic mutations, and/or shifts in the clonal architecture of these lesions.

Mutations in the chromatin remodeling complex, specifically *ARID1A, ARID1B*, and *SMARCA4*, have been described in up to 62% of mesonephric and mesonephric-like carcinomas, with 38% of cervical mesonephric carcinomas showing *ARID1A* mutations, in conjunction with *KRAS* mutations [3]. This is similar to our case (CX26) where the mesonephric component harbored both *KRAS* and *ARID1A* mutations. In contrast, the adjacent endometrioid component harbored both *ARID1A* and *CTNNB1* mutations without *KRAS*, as seen in endometrial endometrioid adenocarcinomas. This observation is consistent with the concept of transdifferentiation and lineage plasticity [53]. Also consistent with previous studies [3, 10], we report recurrent gains of chromosomes 1q, 10 and 12 in both mesonephric and mesonephric-like tumors. These alterations have been found to be recurrent and to be associated with poor outcome in endometrioid endometrial carcinoma [24], and to be associated with the presence of metastatic disease in mesonephric and mesonephric-like carcinomas [3, 10]. In our series, given the limited number of sequenced paired primary and metastatic tumors and lack of a formal survival analysis, these results should be interpreted with caution.

Our study has several limitations. All genomic DNA samples included in this study were obtained from formalinfixed and paraffin-embedded tissues, and due to the limited amount of tumor and matched normal tissues, these samples were subjected to massively parallel sequencing targeting cancer-related genes rather than to whole-exome or even whole-genome sequencing. Therefore, we cannot rule out the possibility that additional genes not included in the sequencing panel may be involved in the development and progression of these tumors. Also, mutational signatures could not be inferred due to the small number of somatic mutations identified in these cases. Given the rarity of these tumors, the sample size may have limited the identification of statistically significant differences in the comparisons performed, also, in some cases, the primary tumor was not available for sequencing.

Despite these limitations, our findings demonstrate that, akin to mesonephric carcinomas, mesonephric-like carcinomas are underpinned by recurrent *KRAS* mutations and that mutations affecting RAS/MAPK family genes are likely associated with the development of the disease. Further studies to assess the biological and clinical significance of these alterations in mesonephric and mesonephric-like tumors are warranted. Our findings provide further evidence to support the concept that mesonephric-like carcinomas are derived from a Müllerian substrate, in contrast to cervical mesonephric carcinomas which arise from preexisting Wolffian remnants.

Supplementary Material

Refer to Web version on PubMed Central for supplementary material.

Funding

JSR-F is funded in part by the Breast Cancer Research Foundation, BW in part by Breast Cancer Research Foundation, Cycle for Survival and Stand Up to Cancer grants, FP partially by a National Institutes of Health (NIH)/National Cancer Institute K12 CA184746 grant, and FP, JSR-F, and BW in part by the National Institutes of Health/National Cancer Institute P50 CA247749 01 grant. Research reported in this publication was supported in part by a National Cancer Institute Cancer Center Core Grant No. P30-CA008748.

References

1. Ferry JA, Scully RE. Mesonephric remnants, hyperplasia, and neoplasia in the uterine cervix. A study of 49 cases. Am J Surg Pathol. 1990;14:1100–11. [PubMed: 2252101]
2. Clement PB, Young RH, Keh P, Ostor AG, Scully RE. Malignant mesonephric neoplasms of the uterine cervix. A report of eight cases, including four with a malignant spindle cell component. Am J Surg Pathol. 1995;19:1158–71. [PubMed: 7573674]
3. Mirkovic J, Sholl LM, Garcia E, Lindeman N, MacConaill L, Hirsch M, et al. Targeted genomic profiling reveals recurrent KRAS mutations and gain of chromosome 1q in mesonephric carcinomas of the female genital tract. Mod Pathol. 2015;28:1504–14. [PubMed: 26336887]
4. Shoeir S, Balachandran AA, Wang J, Sultan AH. Mesonephric adenocarcinoma of the vagina masquerading as a suburethral cyst. BMJ Case Rep. 2018;2018:bcr2018224758.
5. Mueller I, Kametriser G, Jacobs VR, Bogner G, Staudach A, Koch H, et al. Mesonephric adenocarcinoma of the vagina: Diagnosis and multimodal treatment of a rare tumor and analysis of worldwide experience. Strahlenther Onkol. 2016;192:668–71. [PubMed: 27349710]
6. Roma AA Mesonephric carcinosarcoma involving uterine cervix and vagina: report of 2 cases with immunohistochemical positivity for PAX2, PAX8, and GATA-3. Int J Gynecol Pathol. 2014;33:624–9. [PubMed: 25272303]
7. Plesinac-Karapandzic V, Stojanovic Rundic S, Jankovic R, Nadrljanski M, Milovanovic Z, Tomasevic A, et al. Non-diethylstilbestrol exposed vaginal adenocarcinoma in young patients associated with unilateral renal agenesis: two case reports and literature review. Eur J Gynaecol Oncol. 2017;38:157–61. [PubMed: 29767889]
8. McFarland M, Quick CM, McCluggage WG. Hormone receptor-negative, thyroid transcription factor 1-positive uterine and ovarian adenocarcinomas: report of a series of mesonephric-like adenocarcinomas. Histopathology. 2016;68:1013–20. [PubMed: 26484981]
9. Kenny SL, McBride HA, Jamison J, McCluggage WG. Mesonephric adenocarcinomas of the uterine cervix and corpus: HPV-negative neoplasms that are commonly PAX8, CA125, and HMGA2 positive and that may be immunoreactive with TTF1 and hepatocyte nuclear factor 1-beta. Am J Surg Pathol. 2012;36:799–807. [PubMed: 22456609]
10. Na K, Kim HS. Clinicopathologic and molecular characteristics of mesonephric adenocarcinoma arising from the uterine body. Am J Surg Pathol. 2019;43:12–25. [PubMed: 29189288]
11. Mirkovic J, McFarland M, Garcia E, Sholl LM, Lindeman N, MacConaill L, et al. Targeted genomic profiling reveals recurrent KRAS mutations in mesonephric-like adenocarcinomas of the female genital tract. Am J Surg Pathol. 2018;42:227–33. [PubMed: 28984674]
12. Wu H, Zhang L, Cao W, Hu Y, Liu Y. Mesonephric adenocarcinoma of the uterine corpus. Int J Clin Exp Pathol. 2014;7:7012–9. [PubMed: 25400789]
13. Bague S, Rodriguez IM, Prat J. Malignant mesonephric tumors of the female genital tract: a clinicopathologic study of 9 cases. Am J Surg Pathol. 2004;28:601–7. [PubMed: 15105647]
14. Meguro S, Yasuda M, Shimizu M, Kurosaki A, Fujiwara K. Mesonephric adenocarcinoma with a sarcomatous component, a notable subtype of cervical carcinosarcoma: a case report and review of the literature. Diagn Pathol. 2013;8:74. [PubMed: 23651629]
15. McCluggage WG, Vosmikova H, Laco J. Ovarian combined low-grade serous and mesonephric-like adenocarcinoma: further evidence for a mullerian origin of mesonephric-like adenocarcinoma. Int J Gynecol Pathol. 2020;39:84–92. [PubMed: 30575604]
16. Chapel DB, Joseph NM, Krausz T, Lastra RR. An ovarian adenocarcinoma with combined low-grade serous and mesonephric morphologies suggests a mullerian origin for some mesonephric carcinomas. Int J Gynecol Pathol. 2018;37:448–59. [PubMed: 28863071]
17. Dundr P, Gregova M, Nemejcova K, Bartu M, Hajkova N, Hojny J, et al. Ovarian mesonephric-like adenocarcinoma arising in serous borderline tumor: a case report with complex morphological and molecular analysis. Diagn Pathol. 2020;15:91. [PubMed: 32693840]
18. Yano M, Shintani D, Katoh T, Hamada M, Ito K, Kozawa E, et al. Coexistence of endometrial mesonephric-like adenocarcinoma and endometrioid carcinoma suggests a Mullerian duct lineage: a case report. Diagn Pathol. 2019;14:54. [PubMed: 31174566]

19. Howitt BE, Nucci MR. Mesonephric proliferations of the female genital tract. Pathology. 2018;50:141–50. [PubMed: 29269124]
20. Pors J, Cheng A, Leo JM, Kinloch MA, Gilks B, Hoang L. A comparison of GATA3, TTF1, CD10, and calretinin in identifying mesonephric and mesonephric-like carcinomas of the gynecologic tract. Am J Surg Pathol. 2018;42:1596–606. [PubMed: 30148742]
21. Howitt BE, Emori MM, Drapkin R, Gaspar C, Barletta JA, Nucci MR, et al. GATA3 is a sensitive and specific marker of benign and malignant mesonephric lesions in the lower female genital tract. Am J Surg Pathol. 2015;39:1411–9. [PubMed: 26135559]
22. Euscher ED, Bassett R, Duose DY, Lan C, Wistuba I, Ramondetta L, et al. Mesonephric-like carcinoma of the endometrium: a subset of endometrial carcinoma with an aggressive behavior. Am J Surg Pathol. 2020;44:429–43. [PubMed: 31725471]
23. Kolin DL, Costigan DC, Dong F, Nucci MR, Howitt BE. A combined morphologic and molecular approach to retrospectively identify KRAS-mutated mesonephric-like adenocarcinomas of the endometrium. Am J Surg Pathol. 2019;43:389–98. [PubMed: 30489318]
24. Kandoth C, Schultz N, Cherniack AD, Akbani R, Liu Y, Cancer Genome Atlas Research Network, et al.. Integrated genomic characterization of endometrial carcinoma. Nature. 2013;497:67–73. [PubMed: 23636398]
25. Kurman RJCM, Herrington CS, Young RH. WHO classification of tumours of female reproductive organs. Vol. 6, 4th ed. Lyon, France: IARC; 2014.
26. Pecorelli S Revised FIGO staging for carcinoma of the vulva, cervix, and endometrium. Int J Gynaecol Obstet. 2009;105:103–4. [PubMed: 19367689]
27. Da Cruz Paula A, da Silva EM, Segura SE, Pareja F, Bi R, Selenica P, et al. Genomic profiling of primary and recurrent adult granulosa cell tumors of the ovary. Mod Pathol. 2020;33:1606–17. [PubMed: 32203090]
28. Weigelt B, Bi R, Kumar R, Blecua P, Mandelker DL, Geyer FC, et al. The landscape of somatic genetic alterations in breast cancers from ATM germline mutation carriers. J Natl Cancer Inst. 2018;110:1030–4. [PubMed: 29506079]
29. Geyer FC, Li A, Papanastasiou AD, Smith A, Selenica P, Burke KA, et al. Recurrent hotspot mutations in HRAS Q61 and PI3K-AKT pathway genes as drivers of breast adenomyoepitheliomas. Nat Commun. 2018;9:1816. [PubMed: 29739933]
30. Cheng DT, Mitchell TN, Zehir A, Shah RH, Benayed R, Syed A, et al. Memorial Sloan Kettering-Integrated Mutation Profiling of Actionable Cancer Targets (MSK-IMPACT): a hybridization capture-based next-generation sequencing clinical assay for solid tumor molecular oncology. J Mol Diagn. 2015;17:251–64. [PubMed: 25801821]
31. Kim SH, Da Cruz Paula A, Basili T, Dopeso H, Bi R, Pareja F, et al. Identification of recurrent FHL2-GLI2 oncogenic fusion in sclerosing stromal tumors of the ovary. Nat Commun. 2020;11:44. [PubMed: 31896750]
32. Cibulskis K, Lawrence MS, Carter SL, Sivachenko A, Jaffe D, Sougnez C, et al. Sensitive detection of somatic point mutations in impure and heterogeneous cancer samples. Nat Biotechnol. 2013;31:213–9. [PubMed: 23396013]
33. Saunders CT, Wong WS, Swamy S, Becq J, Murray LJ, Cheetham RK. Strelka: accurate somatic small-variant calling from sequenced tumor-normal sample pairs. Bioinformatics. 2012;28:1811–7. [PubMed: 22581179]
34. Koboldt DC, Zhang Q, Larson DE, Shen D, McLellan MD, Lin L, et al. VarScan 2: somatic mutation and copy number alteration discovery in cancer by exome sequencing. Genome Res. 2012;22:568–76. [PubMed: 22300766]
35. Narzisi G, Corvelo A, Arora K, Bergmann EA, Shah M, Musunuri R, et al. Genome-wide somatic variant calling using localized colored de Bruijn graphs. Commun Biol. 2018;1:20. [PubMed: 30271907]
36. Narzisi G, O'Rawe JA, Iossifov I, Fang H, Lee YH, Wang Z, et al. Accurate de novo and transmitted indel detection in exome-capture data using microassembly. Nat Methods. 2014;11:1033–6. [PubMed: 25128977]
37. Li H, Handsaker B, Wysoker A, Fennell T, Ruan J, Homer N, et al. The sequence alignment/map format and SAMtools. Bioinformatics. 2009;25:2078–9. [PubMed: 19505943]

38. Shen R, Seshan VE. FACETS: allele-specific copy number and clonal heterogeneity analysis tool for high-throughput DNA sequencing. Nucleic Acids Res. 2016;44:e131. [PubMed: 27270079]
39. Carter SL, Cibulskis K, Helman E, McKenna A, Shen H, Zack T, et al. Absolute quantification of somatic DNA alterations in human cancer. Nat Biotechnol. 2012;30:413–21. [PubMed: 22544022]
40. Pareja F, Lee JY, Brown DN, Piscuoglio S, Gularte-Merida R, Selenica P, et al. The genomic landscape of mucinous breast cancer. J Natl Cancer Inst. 2019;111:737–41. [PubMed: 30649385]
41. Chang MT, Bhattarai TS, Schram AM, Bielski CM, Donoghue MTA, Jonsson P, et al. Accelerating discovery of functional mutant alleles in cancer. Cancer Disco. 2018;8:174–83.
42. Weigelt B, Vargas HA, Selenica P, Geyer FC, Mazaheri Y, Blecua P, et al. Radiogenomics analysis of intratumor heterogeneity in a patient with high-grade serous ovarian cancer. JCO Precis Oncol. 2019;3:PO.18.00410.
43. Horn LC, Hohn AK, Krucken I, Stiller M, Obeck U, Brambs CE. Mesonephric-like adenocarcinomas of the uterine corpus: report of a case series and review of the literature indicating poor prognosis for this subtype of endometrial adenocarcinoma. J Cancer Res Clin Oncol. 2020;146:971–83. [PubMed: 31927619]
44. Canon J, Rex K, Saiki AY, Mohr C, Cooke K, Bagal D, et al. The clinical KRAS(G12C) inhibitor AMG 510 drives anti-tumour immunity. Nature. 2019;575:217–23. [PubMed: 31666701]
45. Hallin J, Engstrom LD, Hargis L, Calinisan A, Aranda R, Briere DM, et al. The KRAS(G12C) inhibitor MRTX849 provides insight toward therapeutic susceptibility of KRAS-mutant cancers in mouse models and patients. Cancer Disco. 2020;10:54–71.
46. Hong DS, Fakih MG, Strickler JH, Desai J, Durm GA, Shapiro GI, et al. KRAS(G12C) inhibition with sotorasib in advanced solid tumors. N Engl J Med. 2020;383:1207–17. [PubMed: 32955176]
47. Basho RK, Gilcrease M, Murthy RK, Helgason T, Karp DD, Meric-Bernstam F, et al. Targeting the PI3K/AKT/mTOR pathway for the treatment of mesenchymal triple-negative breast cancer: evidence from a phase 1 trial of mTOR inhibition in combination with liposomal doxorubicin and bevacizumab. JAMA Oncol. 2017;3:509–15. [PubMed: 27893038]
48. Montalvo N, Redroban L, Galarza D. Mesonephric adenocarcinoma of the cervix: a case report with a three-year follow-up, lung metastases, and next-generation sequencing analysis. Diagn Pathol. 2019;14:71. [PubMed: 31266530]
49. Goyal A, Yang B. Differential patterns of PAX8, p16, and ER immunostains in mesonephric lesions and adenocarcinomas of the cervix. Int J Gynecol Pathol. 2014;33:613–9. [PubMed: 25272301]
50. Kir G, Seneldir H, Kiran G. A case of mesonephric adenocarcinoma of the uterine cervix mimicking an endometrial clear cell carcinoma in the curettage specimen. J Obstet Gynaecol. 2016;36:827–9. [PubMed: 27147080]
51. Cavalcanti MS, Schultheis AM, Ho C, Wang L, DeLair DF, Weigelt B, et al. Mixed mesonephric adenocarcinoma and high-grade neuroendocrine carcinoma of the uterine cervix: case description of a previously unreported entity with insights into its molecular pathogenesis. Int J Gynecol Pathol. 2017; 36:76–89. [PubMed: 27532149]
52. Stolnicu S, Barsan I, Hoang L, Patel P, Terinte C, Pesci A, et al. International endocervical adenocarcinoma criteria and classification (IECC): a new pathogenetic classification for invasive adenocarcinomas of the endocervix. Am J Surg Pathol. 2018;42:214–26. [PubMed: 29135516]
53. Quintanal-Villalonga A, Chan JM, Yu HA, Pe'er D, Sawyers CL, Sen T, et al. Lineage plasticity in cancer: a shared pathway of therapeutic resistance. Nat Rev Clin Oncol. 2020;17:360–71. [PubMed: 32152485]

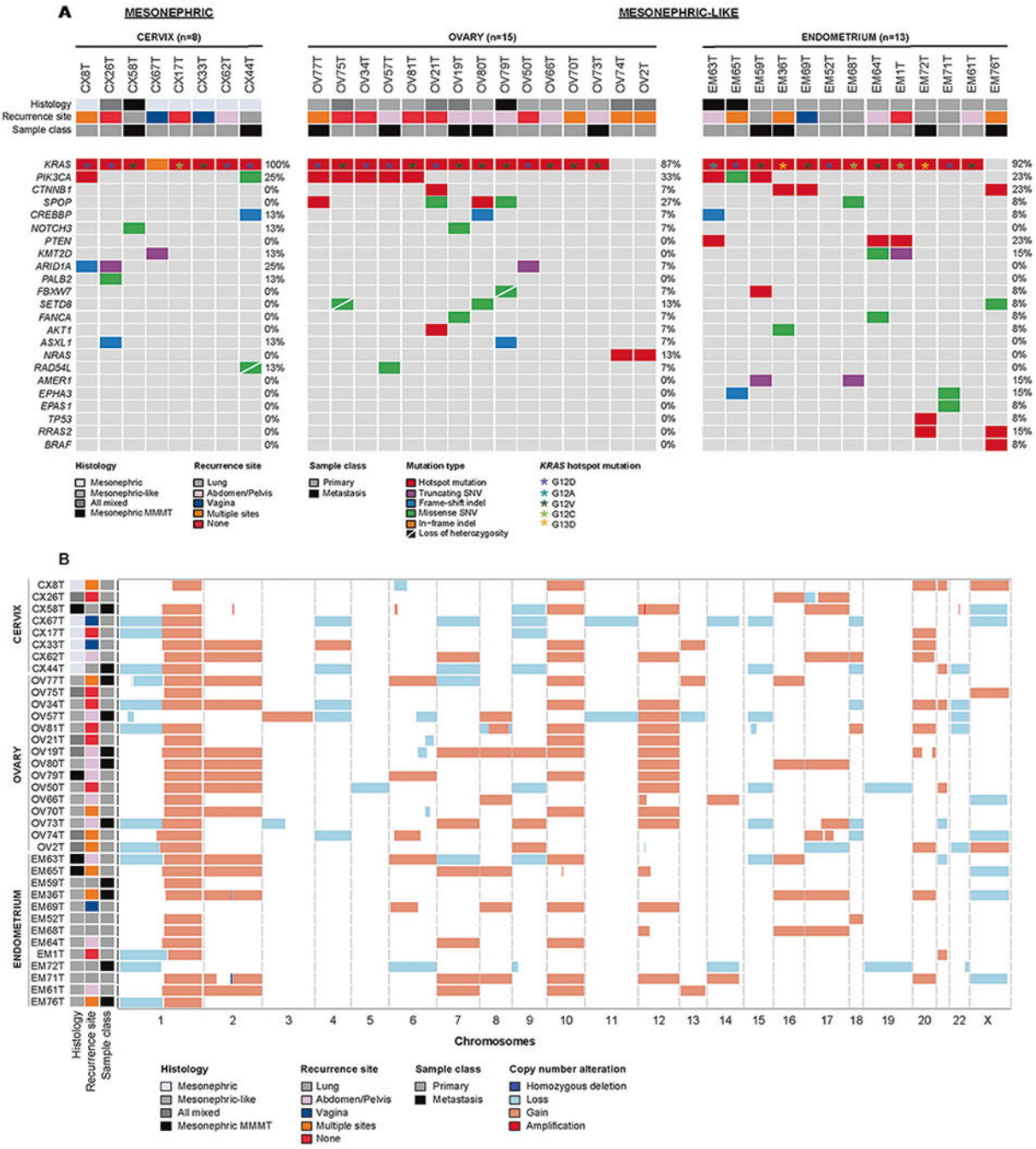

Fig. 1. Mutational profiles and copy number alterations of cervical mesonephric carcinomas and mesonephric-like carcinomas of the ovary and endometrium.

A Non-synonymous somatic mutations identified in 8 mesonephric and 28 mesonephric-like carcinomas detected by massively parallel sequencing targeting 468 cancer-related genes. Cases are shown in columns and genes in rows. Clinicopathologic characteristics including histology, recurrence site, and primary/metastasis are depicted in phenobars (top). Somatic mutation types are color-coded according to the legend. Loss of heterozygosity (LOH) of the wild-type allele is displayed by a diagonal bar. Please note that for cases with mixed

histology only the mesonephric or the mesonephric-like components are shown. **B** Copy number alterations in the 8 mesonephric and 28 mesonephric-like carcinomas subjected to targeted MSK-IMPACT massively parallel sequencing. Cases are shown in rows and chromosomes in columns along the *x*-axis. Clinicopathologic characteristics including histology, recurrence site, and primary/metastasis are depicted in the phenobar (left). Light red, copy number gain; light blue, copy number loss; white, no change. No recurrent amplifications or homozygous deletions were identified.

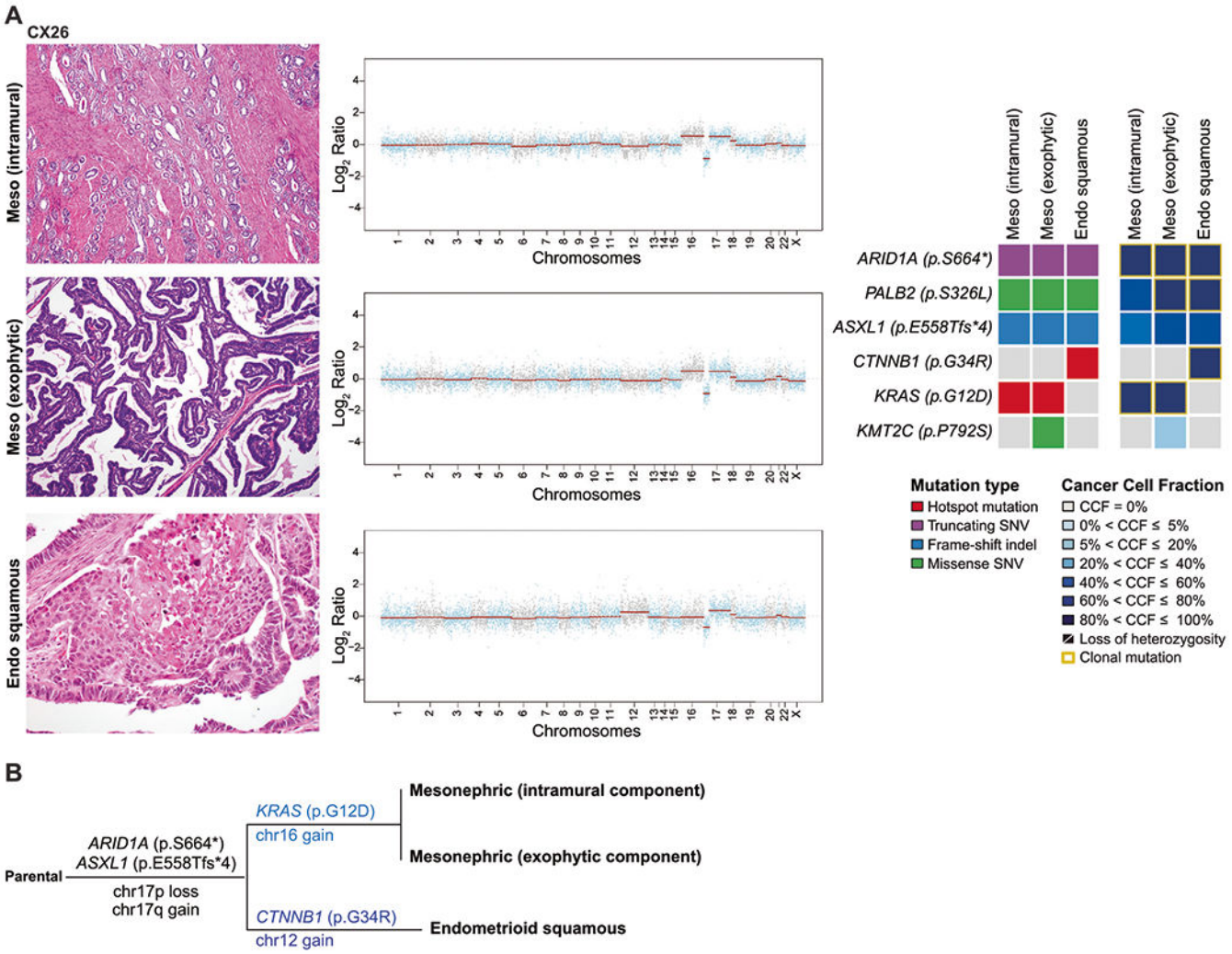

Fig. 2. Gene copy number alterations and somatic mutations identified in histologically distinct components of the mixed mesonephric and endometrioid carcinoma CX26.

Representative hematoxylin and eosin-stained sections of the histologically distinct components of CX26 (**A**), including mesonephric (top left), mesonephric exophytic (middle left), and endometrioid squamous (bottom left) components. Corresponding copy number plots of each component are shown (middle) with Log_2-ratios on the *y*-axis and chromosome location on the *x*-axis. On the right, heatmaps depicting non-synonymous somatic mutations (left) and the cancer cell fractions of the mutations identified (right) in both histological components. **B** Maximum parsimony tree depicting the clonal evolution of the separate components of CX26. The branches are representative of each of the clones identified and selected somatic mutations and gene copy number alterations that define a given clone are illustrated along the branches. The length of the branches is representative of the number of somatic mutations and/or copy number alterations that distinguish a given clone from its ancestral clone.

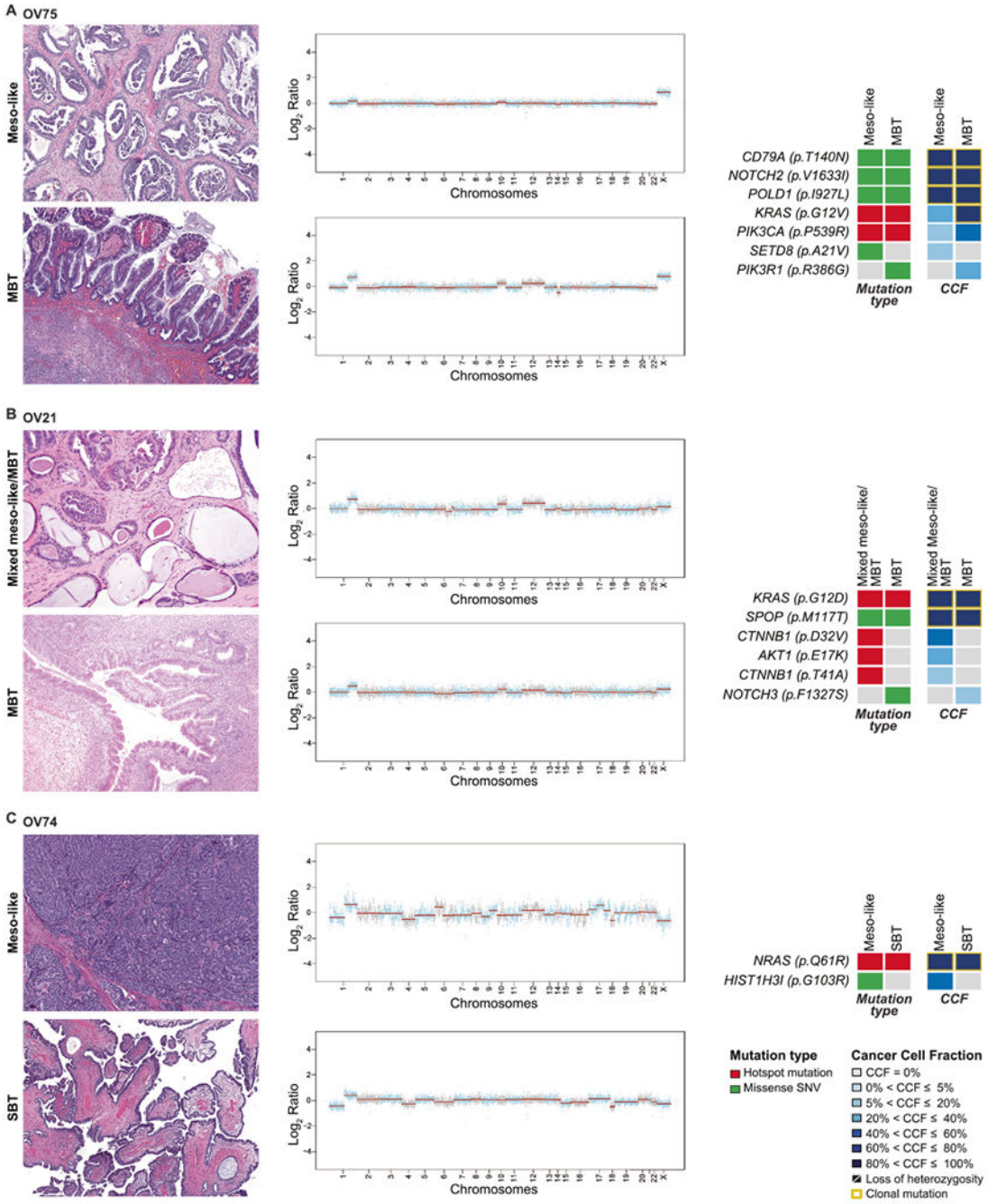

Fig. 3. Somatic mutations and copy number alterations identified in the mesonephric-like carcinoma of the ovary mixed with mucinous and serous tumors.

Representative hematoxylin and eosinstained sections of separate components of mixed mesonephric-like and mucinous borderline tumors **A** OV75 and **B** OV21; and **C** OV74 mixed mesonephric-like and serous borderline tumor/low-grade serous carcinoma (SBT/LGSC) are shown (left). Corresponding copy number plots are shown (middle) with Log_2-ratios on the *y*-axis and chromosome location on the *x*-axis. On the right, heatmaps depicting non-synonymous somatic mutations (left) and the cancer cell fractions of the

mutations identified (right) in both histological components. Clonal mutations are depicted by a yellow box. Cancer cell fractions are color-coded according to the legend.

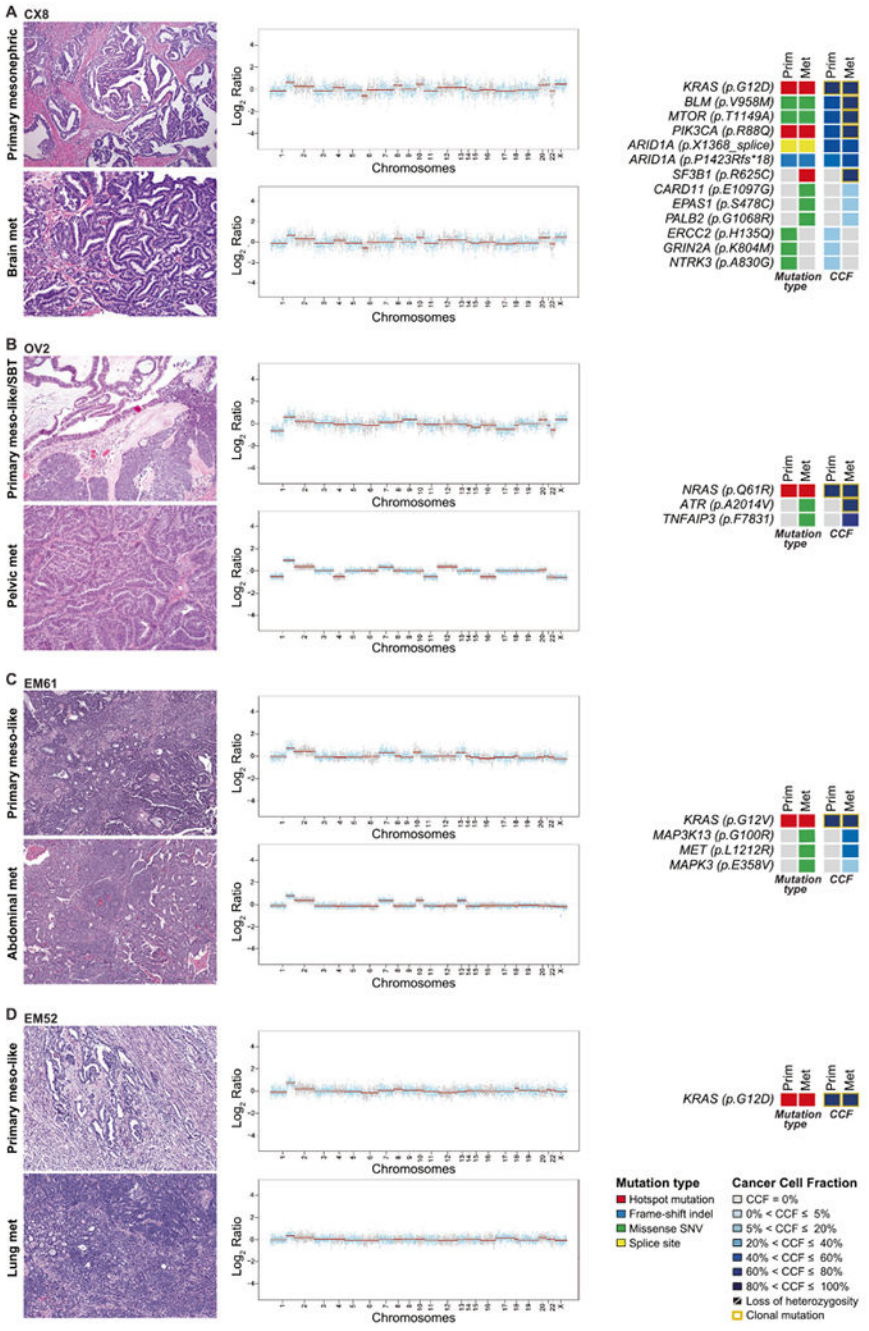

Fig. 4. Gene copy number alterations and somatic mutations identified in primary and matched metastatic mesonephric and endometrial/ovarian mesonephric-like carcinomas.

Representative hematoxylin and eosin micrographs of matched primary and metastatic tumor of one mesonephric (CX8) carcinoma (**A**), one ovarian mixed mesonephric-like with serous borderline tumor (OV2) (**B**), two endometrial mesonephric-like carcinomas: EM61 (**C**), and EM52 (**D**) are shown (left). Chromosome plots are shown on the right, with the Log_2-ratios plotted on the *y*-axis according to their genomic coordinates on the *x*-axis. Non-synonymous somatic mutations and the cancer cell fractions of the mutations are shown.

Clonal mutations are depicted by a yellow box. Cancer cell fractions are color-coded according to the legend.

Table 1

Clinicopathologic features of mesonephric and mesonephric-like carcinomas.

Site of origin	Case ID	Age at diagnosis (years)	FIGO stage (2009)	Sample class	Tumor size (cm)	Tumor histology	Recurrence site
Mesonephric cervix	CX8	65	IB1	Primary	2.3	Mesonephric	Liver, brain
	CX17	43	IIB	Primary	4.3	Mesonephric	–
	CX26	30	IB1	Primary	8.6	Mixed mesonephric and endometrioid	–
	CX33	75	IB	Primary	4.7	Mesonephric	Vagina
	CX44	51	IB1	Metastasis (lung)	N/A	Mesonephric	Lung
	CX58	72	IIB	Metastasis (lung)	6.4	Mesonephric carcinosarcoma	Lung
	CX62	70	IV	Primary	8.5	Mesonephric	Pelvis
	CX67	55	IIA	Primary	2.0	Mesonephric	Vagina
Mesonephric-like ovary	OV2	66	IIIC	Primary	5.4	Mixed mesonephric-like and serous borderline tumor	Left rectal mesentery
	OV19	62	N/A	Metastasis (bowel)	7.5	Mixed mesonephric-like and low-grade serous carcinoma	Bowel
	OV21	52	IA	Primary	18.5	Mixed mesonephric-like and mucinous borderline tumor	–
	OV34	76	IVB	Primary	13.1	Mesonephric-like	–
	OV50	67	N/A	Primary	N/A	Mesonephric-like	–
	OV57	66	IIB	Metastasis (pelvic recurrence)	4.0	Mesonephric-like	Pelvis
	OV66	45	IIIA	Primary	18.0	Mesonephric-like	Ovary, lymph node
	OV70	54	IIIC	Primary	15.1	Mesonephric-like	Lung, liver
	OV73	63	IV	Metastasis (liver)	N/A	Mesonephric-like	Liver
	OV74	61	IV	Primary	4.1	Mixed mesonephric-like and serous borderline tumor/low-grade serous carcinoma	Peritoneal and omental carcinomatosis, lung, bowel, liver, abdominal and intrathoracic lymph nodes
	OV75	60	IC	Primary	10.1	Mixed mesonephric-like and mucinous borderline tumor	–
	OV77	36	IA	Metastasis (lung)	14.0	Mesonephric-like	Lung, pubic bone
	OV79	76	IC	Primary	3.5	Mesonephric-like carcinosarcoma	Iliopsoas
	OV80	59	IIB	Metastasis (bladder)	N/A	Mesonephric-like	Bladder
	OV81	71	IC	Primary	8.0	Mesonephric-like	–

Mod Pathol. Author manuscript; available in PMC 2022 February 01.

Site of origin	Case ID	Age at diagnosis (years)	FIGO stage (2009)	Sample class	Tumor size (cm)	Tumor histology	Recurrence site
Mesonephric-like endometrium	EM1	71	IIIC	Primary	3.0	Mesonephric-like	–
	EM36	60	IIIC	Metastasis (brain)	4.5	Mesonephric-like	Lung, brain
	EM52	57	IB	Primary	2.8	Mesonephric-like	Lung
	EM59	51	IC	Metastasis (lung)	3.5	Mesonephric-like	Lung
	EM61	58	IA	Primary	4.5	Mesonephric-like	Lymph nodes, abdomen
	EM63	67	IVA	Primary	5.7	Mesonephric-like carcinosarcoma	Abd pelvic
	EM64	62	IA	Primary	3.0	Mesonephric-like	Pelvic lymph nodes, omentum
	EM65	59	IA	Primary	7.5	Mesonephric-like carcinosarcoma	Bone, liver
	EM68	61	IV	Primary	4.0	Mesonephric-like	Lung
	EM69	48	IA	Primary	2.6	Mesonephric-like	Vagina apex
	EM71	58	N/A	Primary	N/A	Mesonephric-like	Lung
	EM72	52	IV	Metastasis (lung)	8.0	Mesonephric-like	Lung
	EM76	61	IV	Metastasis (vaginal recurrence)	10.5	Mesonephric-like	Vagina, lung

FIGO International Federation of Gynecology and Obstetrics, *N/A* not available.

Mod Pathol. Author manuscript; available in PMC 2022 February 01.

Table 2

Immunohistochemical findings of mesonephric and mesonephric-like carcinomas.

Site of origin	Case ID	Tumor histology	Histologic component	PAX8	CK7	GATA3	TTF-1	ER	PR	Calretinin	CD10	WT1	p53	MMR	HNF1b	CK20
Mesonephric cervix	CX8	Mesonephric		P	P			N	N	P	P	N	WT		N	
	CX17	Mesonephric														
	CX26	Mixed mesonephric and endometrioid	Mesonephric			N	N	N	N		P			R		
			Endometrioid			N	N	P	P							
	CX33	Mesonephric		P				N	N	P	N		WT			
	CX44	Mesonephric			N		N	N	N	P						
	CX58	Mesonephric carcinosarcoma		P		P	N	N		P	P		WT	R		
	CX62	Mesonephric		P	P	P	N	N	N	N	P	N	WT		N	
	CX67	Mesonephric						N	N					R		
Mesonephric-like ovary	OV2	Mixed mesonephric-like and serous borderline tumor	Mesonephric	P		P	P	N	N	N		N	WT	R		N
			Serous									P	WT			
	OV19	Mixed mesonephric-like and low-grade serous carcinoma	Mesonephric	P		P	N	N		N	N	N			N	
			Serous	P				P				P				
	OV21	Mixed mesonephric-like and mucinous borderline tumor	Mesonephric	P	P	P	P	N	N	N	P	N			P	N
			Mucinous	P	P	N	N									P
	OV34	Mesonephric-like		P		P	P	N	N			N	WT	R		
	OV50	Mesonephric-like		P	P	P	P	N	N	N	P	N	WT	R	P	
	OV57	Mesonephric-like		P		P	P	N						R		
	OV66	Mesonephric-like		P	P	P	P	N	N	N	N	N	WT	R	P	N
	OV70	Mesonephric-like					P	N								
	OV73	Mesonephric-like		P	P	P	P	F	N	N	N	N		R		N
	OV74	Mixed mesonephric-like and serous borderline tumor/low-grade serous carcinoma	Mesonephric	P	P	N	P	N	N	P		N			P	
			Serous	P	P	N	N	P	P	N		P			P	
	OV75	Mixed mesonephric-like and mucinous borderline tumor	Mesonephric	P	P	P	P	F	N			N	WT	R		N

Site of origin	Case ID	Tumor histology	Histologic component	PAX8	CK7	GATA3	TTF-1	ER	PR	Calretinin	CD10	WT1	p53	MMR	HNF1b	CK20
			Mucinous	P	P	P	P	N	N			N	WT	R		P
	OV77	Mesonephric-like		P			N	N	N			N	WT	R		
	OV79	Mesonephric-like carcinosarcoma		P	N		N	N								N
	OV80	Mesonephric-like		P	P	P	P	N	N	P		N			N	
	OV81	Mesonephric-like		P		P	N	N	N			N	WT			
Mesonephric-like endometrium	EMI	Mesonephric-like		P		N	F	N	N							
	EM36	Mesonephric-like					P	N	N	N	N	N				
	EM52	Mesonephric-like		P	P	P	N	N	N		P		WT	R	N	N
	EM59	Mesonephric-like		P		P	P	N	N	N	P			R		
	EM61	Mesonephric-like		P			N	N	N	N	N		R	N		
	EM63	Mesonephric-like carcinosarcoma						N					R			
	EM64	Mesonephric-like				P	N	N	N			WT	R			
	EM65	Mesonephric-like carcinosarcoma						N					R			
	EM68	Mesonephric-like		P	P		P	N	N	N		WT			N	
	EM69	Mesonephric-like				P	P	N	N	N		WT	R	N		
	EM71	Mesonephric-like		P	P		N	N	N			WT	R		N	
	EM72	Mesonephric-like		P		P		N	N		N		R	N		
	EM76	Mesonephric-like		P	P			F		N		WT	R			

ER estrogen receptor, *F* focal, *MMR* DNA mismatch repair proteins, *N* negative, *P* positive, *PR* progesterone receptor, *R* retained, *WT* wild-type. *Blank* not performed.

Table 3

Mesonephric and mesonephric-like carcinomas with mixed histology, and primary tumors and matched metastases that were microdissected and analyzed separately.

	Case ID	Sample description	Tumor site of origin
Distinct components from cases with mixed histology	CX26	Endometrioid squamous	Cervix
		Mesonephric exophytic	
		Mesonephric	
	OV21	Mixed mesonephric-like and mucinous borderline tumor	Ovary
		Mucinous borderline tumor	
	OV74	Mesonephric-like	Ovary
		Serous borderline tumor	
	OV75	Mesonephric-like	Ovary
		Mucinous borderline tumor	
Primary and matched metastasis	OV2	Primary mixed mesonephric-like and serous borderline tumor	Ovary
		Pelvic metastasis	
	CX8	Primary mesonephric	Cervix
		Brain metastasis	
	EM52	Primary mesonephric-like tumor	Endometrium
		Lung metastasis	
	EM61	Primary mesonephric-like tumor	Endometrium
		Rectus abdominis metastasis	